

PAPER • OPEN ACCESS

Identification of temperature and diffusion effects during helium swelling of the surface layer of a TiTaNbV alloy

To cite this article: Sholpan G Giniyatova *et al* 2024 *Mater. Res. Express* **11** 076516

View the [article online](#) for updates and enhancements.

You may also like

- [Bi₂Mo₂TiTaO₉ \(M = La or Nd\) Ceramics with High Mechanical Quality Factor Q_m](#)
Muneyasu Suzuki, Hajime Nagata, Jin Ohara et al.
- [Elevating NIR photonic integration with tantalum-niobium pentoxide](#)
Noor Afsary, Md Nasir Uddin, Shariful Islam et al.
- [Impedance and electric modulus study of amorphous TiTaO thin films: highlight of the interphase effect](#)
A Rouahi, A Kahouli, F Challali et al.



The Electrochemical Society
Advancing solid state & electrochemical science & technology

UNITED THROUGH SCIENCE & TECHNOLOGY

**248th
ECS Meeting**
Chicago, IL
October 12-16, 2025
Hilton Chicago



**Science +
Technology +
YOU!**

**SUBMIT
ABSTRACTS by
March 28, 2025**

SUBMIT NOW

Materials Research Express



PAPER

OPEN ACCESS

RECEIVED
15 May 2024REVISED
20 June 2024ACCEPTED FOR PUBLICATION
12 July 2024PUBLISHED
22 July 2024

Original content from this work may be used under the terms of the [Creative Commons Attribution 4.0 licence](#).

Any further distribution of this work must maintain attribution to the author(s) and the title of the work, journal citation and DOI.



Identification of temperature and diffusion effects during helium swelling of the surface layer of a TiTaNbV alloy

Sholpan G Giniyatova¹, Kayrat K Kadyrzhanov^{1,*}, Dmitriy I Shlimas^{1,2}, Daryn B Borgekov^{1,2}, Artem L Kozlovskiy^{1,3} and Vladimir V Uglov^{4,*}¹ Engineering Profile Laboratory, L.N. Gumilyov Eurasian National University, Satpayev St., Astana, 010008, Kazakhstan² Laboratory of Solid State Physics, The Institute of Nuclear Physics, Almaty 050032, Kazakhstan³ Department of General Physics, Satbayev University, Almaty 050032, Kazakhstan⁴ Department of Solid State Physics, Belarusian State University, 220050 Minsk, Belarus

* Authors to whom any correspondence should be addressed.

E-mail: kayrat.kadyrzhanov@mail.ru and vladimir.uglov.bsu@mail.ru**Keywords:** TiTaNbV alloy, structural distortions, deformational swelling, blistering, helium swelling, softening

Abstract

The article presents the comprehensive analysis results of the connection between structural changes caused by the effects of deformation swelling and softening effects during high-dose irradiation with He²⁺ ions, alongside determines the kinetics of changes in structural and strength parameters contingent upon irradiation conditions (in the case of irradiation temperature variations). The interest in such studies is due to the need to study the influence of temperature factors on the diffusion mechanisms of implanted He²⁺ into the damaged layer of a high-entropy TiTaNbV alloy in the case of high-dose irradiation. At the same time, the study of such mechanisms makes it possible to determine not only the radiation resistance of TiTaNbV alloys, but also to expand the general understanding of the influence of the structural features of high-entropy alloys associated with deformation distortion of the crystal structure, which prevents diffusion and migration mechanisms of defect propagation in the damaged layer. During determination of changes in strength properties depending on irradiation conditions, it was found that irradiation temperature growth leads to both a rise in the degree of softening under high-dose irradiation and an increase in the thickness of the softened layer under high-dose irradiation. These changes indicate that at high temperatures, the diffusion of implanted ions is not restrained by structural distortions, which results in their migration to a greater depth exceeding the ion travel depth, which should be considered when designing the use of these alloys in the case of their operation in extreme conditions.

1. Introduction

One of the solutions to the problem associated with the need to reduce the use of fossil resources for energy production, aimed at both solving energy balance issues and solving environmental problems, is the development of alternative methods of energy production, including nuclear energy [1, 2]. The use of traditional technologies in nuclear energy related to the operation of pressurized water reactors, meanwhile, will not fully resolve the issues of the nuclear fuel burnup efficiency growth, and elevate of the environmental friendliness of energy production by reducing the amount of nuclear waste generated during operation [3, 4]. In the last few years, to address these issues, developments in the field of creating high-temperature nuclear reactors capable of operating at elevated temperatures, which makes it possible to increase both the fuel burnup efficiency and the productivity of nuclear power plants, have been actively carried out [5, 6]. At the same time, resolving issues related to the use of high-temperature nuclear reactors is inextricably linked with the search for optimal materials that can withstand extreme operating conditions [7].

Interest in high-entropy alloys based on refractory compounds is due to the great prospects for their use as basic structural materials used under extreme conditions, including temperature heating, as well as radiation

exposure [8–10]. Moreover, considering them as structural materials for nuclear energy, the emphasis is on resistance to the accumulation of radiation damage in the near-surface layers, which are most susceptible to external influences, including mechanical and thermal influences [11, 12]. Unlike conventional alloys, the presence of several elements in equal proportions in high-entropy alloys determines the strength properties, alongside resistance to external influences, due to the formation of a high-strength crystalline structure, which usually has a cubic face-centered or body-centered lattice [13, 14]. It should also be noted that the use of refractory elements such as tantalum, niobium, vanadium, and zirconium [15, 16] in comparison with high-entropy alloys based on elements such as nickel, cobalt, iron, chromium, and aluminum [17, 18] allows the operating temperature growth due to the thermal stability of refractory elements, which, in addition to high strength indicators, also provide resistance to corrosion and degradation in operating conditions at elevated temperatures. At the same time, radiation damage resistance for high-entropy alloys is determined by the presence of structural distortions of the crystal lattice associated with the elemental composition of the alloys, which results in a slowdown in the diffusion of point and vacancy defects in the damaged layer compared to similar effects in austenitic alloys and stainless steels [19, 20]. In this case, structural features associated with the presence of various elements in the composition of the alloys, as well as their equally probable arrangement in the crystal lattice, as a rule, determine the presence of structural distortions, which, as has been shown in a number of works [21–23], provide high strength indicators, and also in the case of radiation damage, restrain migration and diffusion processes, thereby reducing the rate of radiation-induced degradation of the near-surface layer of alloys under long-term exposure. However, in this issue there are still a large number of points that require detailed study and consideration, both from the point of view of a fundamental understanding of the processes of radiation damage in high-entropy alloys, and from a practical point of view associated with conducting full-scale experiments that clearly demonstrate the behavior of materials under irradiation.

The purpose of this study is to determine the influence of the temperature factor on the radiation damage degree in high-entropy TiTaNbV alloys under high-dose irradiation with He^{2+} ions, the use of which makes it possible to simulate the processes of gas swelling of the surface layer, characteristic of extreme operating conditions of such alloys as structural materials in nuclear reactors of new generation Gen IV. The relevance of this study is to determine the influence of irradiation temperature not only on the structural disorder effects caused by the cumulative effects of structural distortions and deformations, but also to determine the diffusion processes on the softening (decrease in hardness) of the surface layer in a TiTaNbV alloy exposed to external influences. Previously, in [23], we carried out a series of experiments to establish the dependence of changes in structural and strength effects in the near-surface layer during helium irradiation of alloy samples with variations in the number of TiTaNbV alloy components. According to the studies, it was determined that the most resistant alloy to radiation embrittlement and swelling under high-dose irradiation with helium ions is the TiTaNbV alloy. However, temperature factors that can lead to the effects of accelerated diffusion of implanted helium in the surface layer of helium were not taken into account, despite the fact that these effects can have a significant impact not only on the degree of radiation damage to the surface layer, but also on its increase in the depth of damage due to diffusion and migration of implanted helium to great depths.

2. Materials and methods

The study of the processes of gas swelling as a result of high-dose irradiation with helium ions (He^{2+}) was conducted in order to determine the connection between the established structural changes (strain distortion of crystal lattice parameters, volumetric swelling, changes in the concentration of defective inclusions) and strength parameters (changes in hardness, strength, dry friction coefficient), alterations in which imply radiation-induced surface erosion processes associated with swelling. The experiments were carried out on samples of high-entropy alloys TiTaNbV with a cubic type of crystal lattice, obtained using the method of arc melting of the elements Ti, Ta, Nb, V in equal stoichiometric ratios [23]. The starting elements were used in the form of powders with a chemical purity of about 99.95%; these powders were purchased from Sigma Aldrich (Sigma, USA). Homogeneity of the alloy composition was achieved by sequential remelting over 5 cycles. Melting was carried out in vacuum (5×10^{-5} mbar) [23]. As a result of similar procedures, TiTaNbV alloys were obtained with a body-centered type of crystal lattice, which has a pronounced textural direction (200), associated with the formation processes of these alloys (see x-ray diffraction results in figure 1). The x-ray diffraction pattern was obtained using a D8 Advance ECO x-ray diffractometer (Bruker, Germany). The diffraction pattern was recorded in the Bragg–Brentano geometry, in the angular range $2\theta = 30^\circ\text{--}110^\circ$, with a step of 0.03° , the acquisition time of the diffraction pattern at a point was 1 s. To generate x-ray radiation, a copper tube with a wavelength $\text{Cu-K}\alpha$, $\lambda = 1.54 \text{ \AA}$ (Current—40 A, tube voltage—25 kV) was used.

The distorted shape of the diffraction reflections, in particular, the pronounced asymmetry of the (200) and (310) reflections, is due to the difference in the atomic radii of the components used for the alloy, which

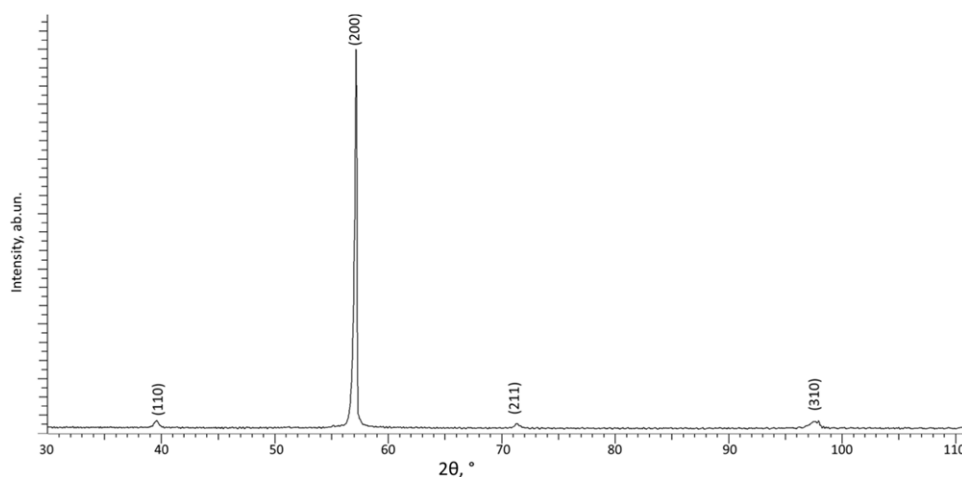


Figure 1. Results of x-ray diffraction of the studied TiTaNbV alloy.

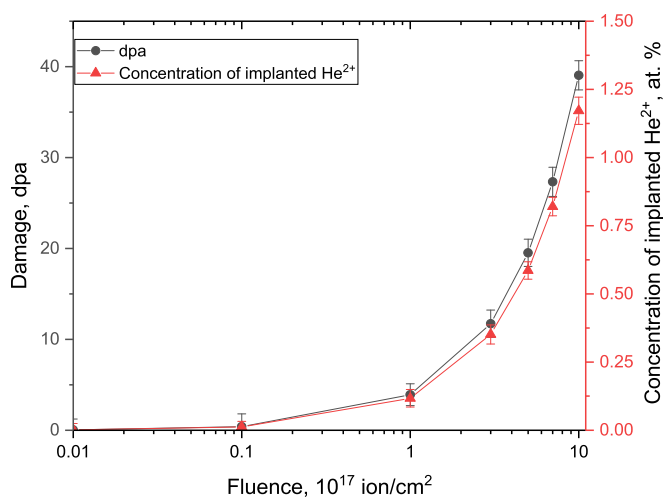


Figure 2. Results of a comparative analysis of changes in the magnitude of atomic displacements and the concentration of implanted ions in the surface layer depending on the irradiation fluence.

determine the presence of deformation distortions in the crystal structure, which in turn determine fairly high radiation resistance [24].

The samples were irradiated at the DC-60 heavy ion accelerator using low-energy helium ions (He^{2+}), the choice of which is determined by the possibilities of modeling the processes of radiation damage associated with the accumulation of slightly soluble helium and its agglomeration in the near-surface layer, as well as caused by this accumulation as a result of agglomeration, swelling and erosion of the surface [23]. In order to determine the influence of temperature factors on the processes of radiation-induced swelling, irradiation experiments were carried out at various temperatures in the range from 300 to 1000 K. Figure 2 illustrates the simulation results of the atomic displacement values and the implanted helium concentration in the near-surface layer, alongside the dependence of the change in the atomic displacement values and the implanted helium concentration, taken at the maximum path length, on the irradiation fluence. Irradiation fluences were chosen from 10^{15} to 1×10^{18} ion cm^{-2} , the use of which made it possible to simulate radiation damage characteristic of atomic displacement values of the order of 40 dpa (at the maximum irradiation fluence, see the data in figure 2). According to simulation data, maximum damage under the selected irradiation conditions can be observed at a depth of about 250–300 nm of the near-surface layer, which is the most vulnerable when these types of materials are used as structural materials. The maximum concentration of implanted helium in the damaged layer that can be achieved with a given irradiation mode is no more than 1.2 at. %. However, at this value, the number of atomic displacements can reach about 40 dpa, which indicates that the main contribution to the change in the structural and strength characteristics of the damaged layer is made by atomic displacements, which are associated with deformation distortion of the crystal structure.

Determination of the influence of various irradiation conditions with variations in irradiation temperature and fluence was carried out by assessment of changes in structural parameters contingent upon variations in irradiation conditions and subsequent determination of the main mechanisms of structural deformation and its influence on the surface layer swelling mechanisms. The assessment was carried out by comparative analysis of alterations in the shape and intensity of the main diffraction reflection (200), the change in which characterizes the deformation distortion of the crystal structure of the damaged layer depending on the conditions of external influences. X-ray diffraction patterns for comparison and determination of the nature of deformation, as well as possible amorphization of the structure under high-dose irradiation, were obtained on a D8 Advance ECO diffractometer (Bruker, Berlin, Germany).

The relationship between structural changes caused by irradiation and a decrease in strength characteristics, in particular, changes in the hardness of the surface layer, was established using the nanoindentation method, which was implemented using a Duroline M1 hardness tester (Metkon, Bursa, Turkey). In this case, the selection of the load on the indenter was carried out taking into account the depth of penetration of ions in the damaged layer, depending on the irradiation conditions. The diffusion mechanisms associated with the migration of implanted helium in the damaged layer above the limit of the depth of penetration of ions into the near-surface layer was determined by measuring the hardness of the samples in depth. For this purpose, measurements were carried out on the side chip of the samples with a step of 50 nm from the surface in order to determine the influence of diffusion processes on the change in hardness under high-dose irradiation. These measurements were carried out for samples irradiated with a maximum fluence of 10^{18} ion cm^{-2} .

Tribological tests aimed at establishing the influence of the accumulation of structural damage and deformations that arose in the near-surface layer as a result of irradiation were carried out using the method of determining the dry friction coefficient, implemented on a Unitest framework SKU UT-750 testing machine (Unitest, USA).

3. Results and discussion

The theory of resistance of high-entropy alloys to radiation damage is based on the assumption of the presence of deformation distortions of the crystal structure that arise due to the presence of various elements that form the crystal lattice by randomly filling positions at the nodes, which leads to the formation of a distorted crystal lattice. Moreover, as is known, thermal exposure in most cases leads to the initialization of relaxation processes [25, 26], leading to partial or complete relaxation of deformation structural distortions, especially if thermal exposure occurs for a long time. In the case of high-temperature irradiation, relaxation processes compete with processes of deformation distortions associated with the processes of interaction of incident ions with the crystal structure of the target, associated with ionization and athermal effects. In this case, thermal effects, under certain conditions, can participate in the relaxation of structural distortions associated with the formation processes of alloys, as well as accelerate the processes of diffusion of implanted ions into the damaged layer, which, as a consequence, will lead to more pronounced structural distortions, as well as increased softening of the surface layer. Moreover, with high-dose irradiation, high concentrations of implanted helium are capable of forming gas-filled bubbles in the form of blisters in the damaged layer, the increase in volume occurs both due to the agglomeration of smaller bubbles into large ones, and due to diffusion processes and high mobility of helium, contributing to an elevation in the helium concentration in the bubble. It is also worth to note that the growth of a bubble (gas-filled cavity) is accompanied by an increase in pressure on the walls, which in turn results in a rise in structural distortions due to deformation swelling of the damaged layer. In turn, in several works [27–29], it was shown that thermal exposure, including post-radiation annealing (especially for steels with metal alloys) leads to an acceleration of the blister formation and bubble growth processes. Such mechanisms are due to the effects of accelerated diffusion, leading to the agglomeration of small bubbles into larger inclusions. A clear confirmation of the influence of irradiation temperature on the mechanisms of blister formation during high-dose irradiation are the images of the surface of alloys exposed to irradiation with a fluence of 10^{18} ion cm^{-2} presented in figure 3. According to the presented images, a change in the irradiation temperature from 300 to 1000 K results in an elevation in the size of the resulting blisters on the surface, which implies helium agglomeration in the resulting cavities. Moreover, in the case of irradiation at 1000 K, a large number of opened blisters are observed with the formation of new blister nuclei of smaller sizes next to the destroyed areas. Such alterations in the surface of alloys observed at elevated temperatures indicate not only the migration processes of helium, which result in a growth in the blister size, but also to an increase in the deformation of the near-surface damaged layer due to both the growth of blisters and the partial destruction of the surface caused by the achievement of critical pressure values in the gas-filled cavity.

Figure 4 shows the results of changes in the position and shape of the main diffraction reflection (200) depending on the irradiation conditions (with variations in fluence and irradiation temperature). According to

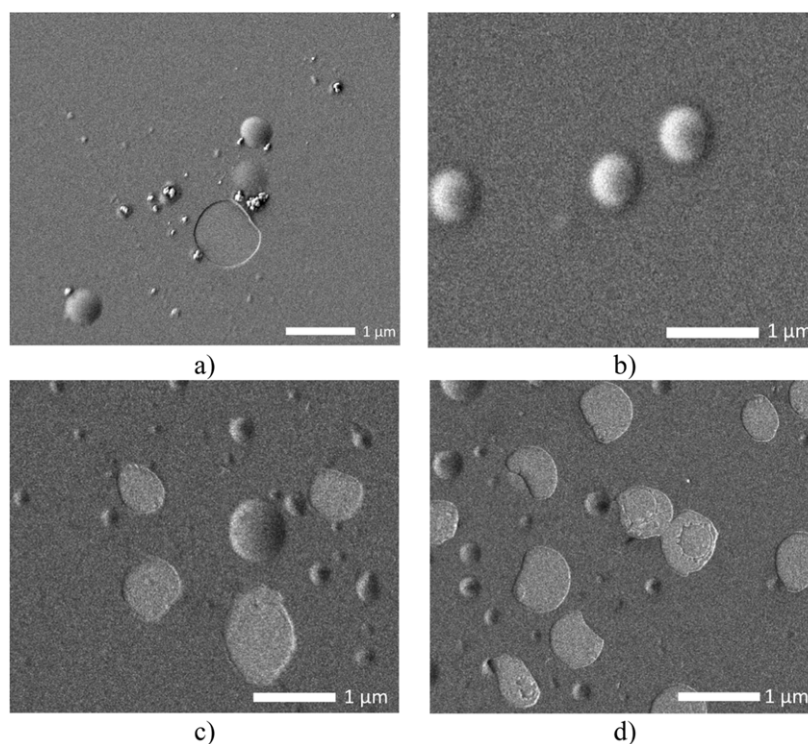


Figure 3. Results of the morphological features of the surface of the TiTaNbV alloy after irradiation with a fluence of 10^{18} ion cm^{-2} in the case of irradiation temperature variation: (a) 300 K; (b) 500 K; (c) 700 K; (d) 1000 K.

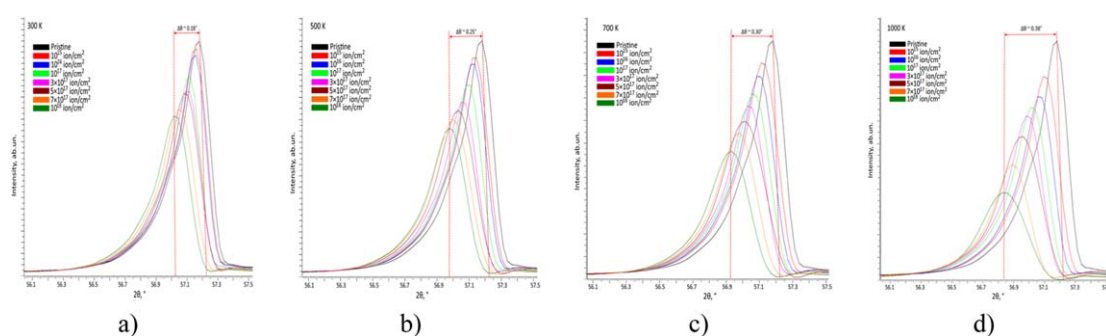
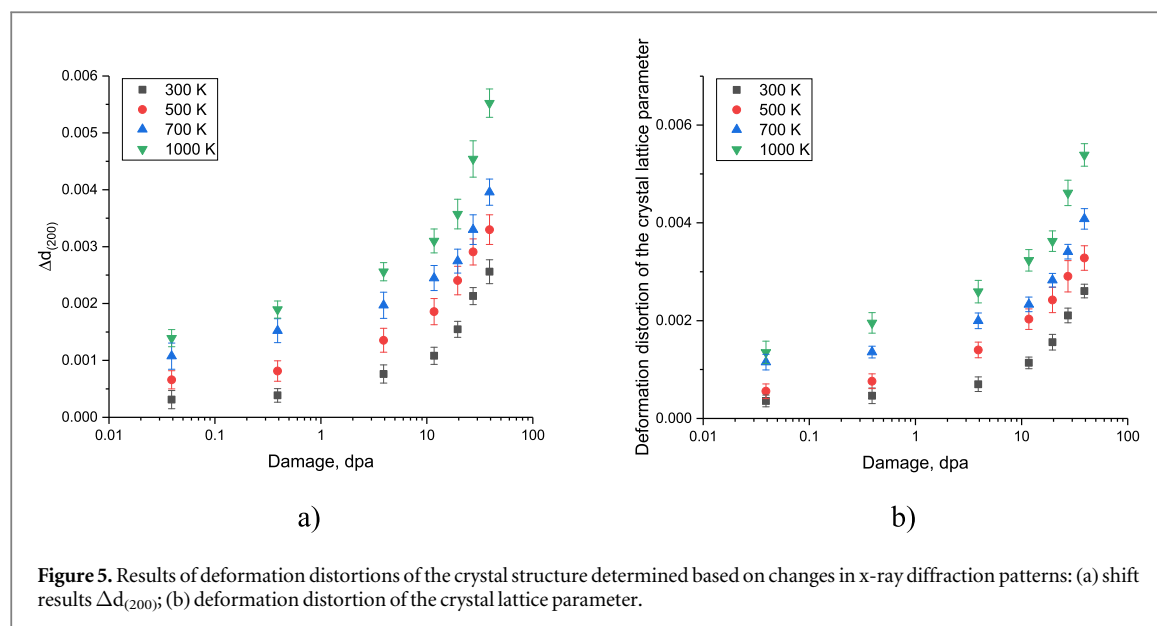


Figure 4. Comparative analysis results of changes in the position and intensity of the diffraction reflection (200) contingent upon the fluence with variations in the irradiation temperature: (a) 300 K; (b) 500 K; (c) 700 K; (d) 1000 K.

the analysis of structural changes, it was determined that there were no new diffraction reflections in the diffraction patterns of the studied samples after the maximum fluence of irradiation, which indicates the absence of recrystallization processes or textural misorientation caused by thermal and athermal effects associated with the processes of interaction of incident ions with the crystal structure of the near-surface layer. The main observed alterations contingent upon irradiation conditions are associated with changes in the intensities of diffraction reflections, and their displacement relative to the initial position, indicating processes of deformation distortion of the crystal structure as a result of irradiation. In this case, a change in irradiation conditions, in particular, an irradiation temperature growth, results in more pronounced shifts in the diffraction reflection alongside its broadening, accompanied by an intensity reduction. Such changes associated with the broadening of reflections under external influences are usually characteristic of the formation of disordered (amorphous) inclusions in the damaged layer caused by severe deformation of the damaged layer under high-dose irradiation.

According to the presented data on changes in the position and shape of the reflex (200), it is clear that the main changes are associated with two factors: a change in position due to a shift to the region of lower 2θ values, indicating an increase in tensile deformation distortions; a change in the FWHM value, which, together with a change in intensity, characterizes the structural ordering degree (the presence of amorphous inclusions associated with the formation of highly disordered regions). In the case of an irradiation temperature of 300 K,



the change in the position of the reflection (200) and its shape is minimal at irradiation fluences of 10^{15} – 10^{17} ion cm^{-2} , and pronounced displacements characteristic of deformation distortion are observed at fluences above 5×10^{17} ion cm^{-2} . At the same time, an increase in the irradiation temperature from 300 to 500 K does not lead to significant changes in the trend of shifts in the position of the reflection, which is characteristic of an increase in deformation microdistortions, the accumulation of which occurs as a result of atomic displacements, as well as migration processes of implanted ions. However, in the case of irradiation temperatures of 700 and 1000 K, the change in the reflection position displacement value is more pronounced in comparison with the data on the value of $\Delta\theta$ obtained for samples irradiated at a temperature of 300 K, and is of the order of $\Delta\theta \sim 0.3^\circ$ – 0.38° , which is 1.5–2.0 times higher than the value $\Delta\theta$ for the maximum irradiation fluence (10^{18} ion cm^{-2}) in the case of irradiation at a temperature of 300 K. It should also be noted that for samples irradiated at temperatures of 700–1000 K, in addition to a growth in the shift value $\Delta\theta$ to the region of small angles, in the case of irradiation fluences above 10^{17} ion cm^{-2} , a strong decrease in intensity and the reflection shape, indicating a rise in the amorphous inclusion concentration, is observed.

Based on the obtained shifts in the position of the diffraction maxima, the values of microdistortions caused by the accumulation of structural distortions in the damaged layer, alongside the processes of helium implantation and its subsequent agglomeration, were determined. Using the obtained dependences of changes in the value of microdistortions on the value of atomic displacements in the damaged layer and irradiation conditions, the main mechanisms of deformation of the damaged layer were determined, as well as the influence of irradiation temperature on the structural disorder degree of the crystal lattice (the results are presented in figure 5(a)). The d_{200} value was refined using the DiffracEVA v.4.2 program code, the use of which makes it possible to establish changes in the value of interplanar distances and angular displacement ($\Delta 2\theta$) of the order of ~ 0.0005 – 0.001 . Such a high accuracy of measurements is due to the high degree of resolution of the obtained diffraction patterns, which reflect minimal changes in the position, shape and intensity of diffraction reflections as a result of external influences.

As can be seen from the data presented, the change in the $\Delta d_{(200)}$ value is characterized by an increase in this value with changes in irradiation conditions (fluence and temperature), which indicates the formation of tensile deformation distortions in the structure, the accumulation of which results in deformation disordering of the damaged layer and its swelling. The nature of deformation microdistortions, meanwhile, is most pronounced for temperatures of 700–1000 K at fluences above 10^{17} ion cm^{-2} , which is in good agreement with the data of morphological features, according to which at high irradiation fluences the formation of gas-filled inclusions, the presence of which is accompanied by deformation distortion of the crystal structure, is observed.

Figure 5(b) reveals the assessment results of the crystal lattice deformation distortion depending on the value of atomic displacements when the irradiation temperature changes, which indicate tensile deformation, leading to the crystal lattice parameter growth under external influences. It should be noted that alterations in irradiation conditions (variations in irradiation temperature) result in different trends in changes in the crystal lattice deformation, which are more pronounced at irradiation temperatures of 700–1000 K, for which pronounced distortions are observed at lower irradiation fluences than in the case of irradiation at temperatures of 300–500 K, for which, at values less than 1 dpa, changes in the deformation distortion value are minimal.

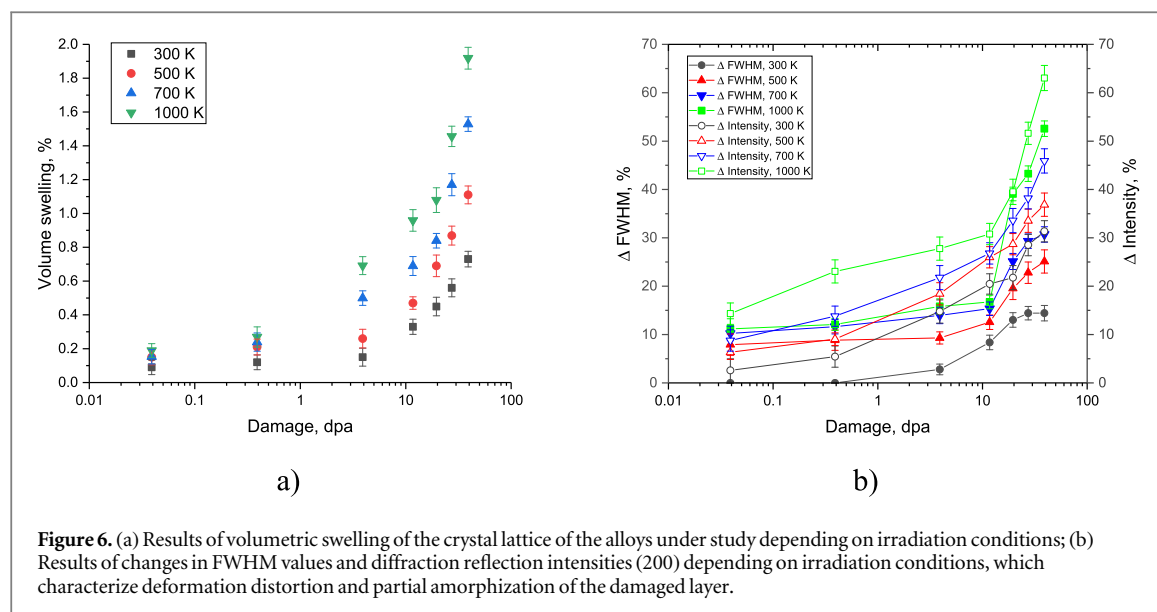


Figure 6. (a) Results of volumetric swelling of the crystal lattice of the alloys under study depending on irradiation conditions; (b) Results of changes in FWHM values and diffraction reflection intensities (200) depending on irradiation conditions, which characterize deformation distortion and partial amorphization of the damaged layer.

Figure 6(a) demonstrates the comparative analysis results of changes in the volumetric swelling of the crystal structure of the alloys under study depending on the irradiation fluence variation (data are presented in terms of the atomic displacement value) and irradiation temperature. The calculations were performed by calculating the value of ΔV , which is the difference in the crystal lattice volumes before and after irradiation under certain conditions.

A change in this value characterizes the deformation swelling of the crystal structure of the damaged near-surface layer as a result of the accumulation of structural distortions caused by irradiation. The nature of changes in this value depending on the irradiation fluence indicates the resistance of alloys to deformation processes, and also characterizes the dynamics of structural disorder when irradiation conditions change. According to the data presented, in the case of irradiation at temperatures of 300 K and 500 K, the main changes, characterized by an exponential increase in the ΔV value, are observed when the atomic displacement value reaches above 10 dpa (at fluences above 3×10^{17} ion cm^{-2}). At the same time, the irradiation temperature growth from 300 K to 500 K results in more intense swelling with an increase in fluence, which is characterized by a difference in the ΔV values at the same dpa values. In the case of irradiation at temperatures of 700 K and 1000 K, a pronounced change in the value of ΔV is observed at a value of 3.9 dpa, which indicates a reduction in the stability of the crystal structure to deformation swelling with the irradiation temperature growth. At the same time, at the maximum irradiation fluence (10^{18} ion cm^{-2}), the difference in ΔV values for alloy samples irradiated at temperatures of 300 K and 1000 K is more than 2.5 times (0.7% for a temperature of 300 K and 1.9% for a temperature of 1000 K). This difference is a direct confirmation that under high-temperature irradiation, diffusion effects leading to accelerated agglomeration and deformation of the crystal structure due to an increase in the volume of gas-filled inclusions become more pronounced, which contributes to the embrittlement of the near-surface layer (see the change in morphological features presented in figure 3). At the same time, a more than twofold change in the ΔV value can result in the damaged layer thickness growth due to more pronounced diffusion of implanted ions, which, due to temperature effects, promotes the migration of defects deeper into the material.

Temperature effects that influence the increase in deformation distortion of the crystal structure, caused by an increase in the size of gas-filled bubbles, as well as their density, were considered in [30]. At the same time, the authors made an assumption about the influence of the composition of the high-entropy alloy on the mechanisms of gas swelling, which is due to the inhibition of the diffusion of implanted helium due to dislocation effects and the presence of point defects. In the case of high irradiation temperatures, relaxation processes associated with the annihilation of point defects and dislocations with temperature changes can lead to a decrease in the concentration of barriers to the diffusion of implanted helium, which in turn explains a more pronounced decrease in the intensity of the diffraction reflection and its broadening, characteristic of amorphization. The results of a comparative analysis of changes in FWHM values and diffraction reflection intensities (200) depending on irradiation conditions, shown in figure 6(b), indicate that the main influence of amorphous inclusions, the accumulation of which occurs due to strong deformation of the near-surface layer near the formed blisters, manifests itself at high irradiation temperatures. In this case, the contribution of changes in the FWHM value and intensity, indicating partial amorphization of the damaged layer, is more pronounced for irradiation temperatures of 700–1000 K, while for a temperature of 300 K, the change in the

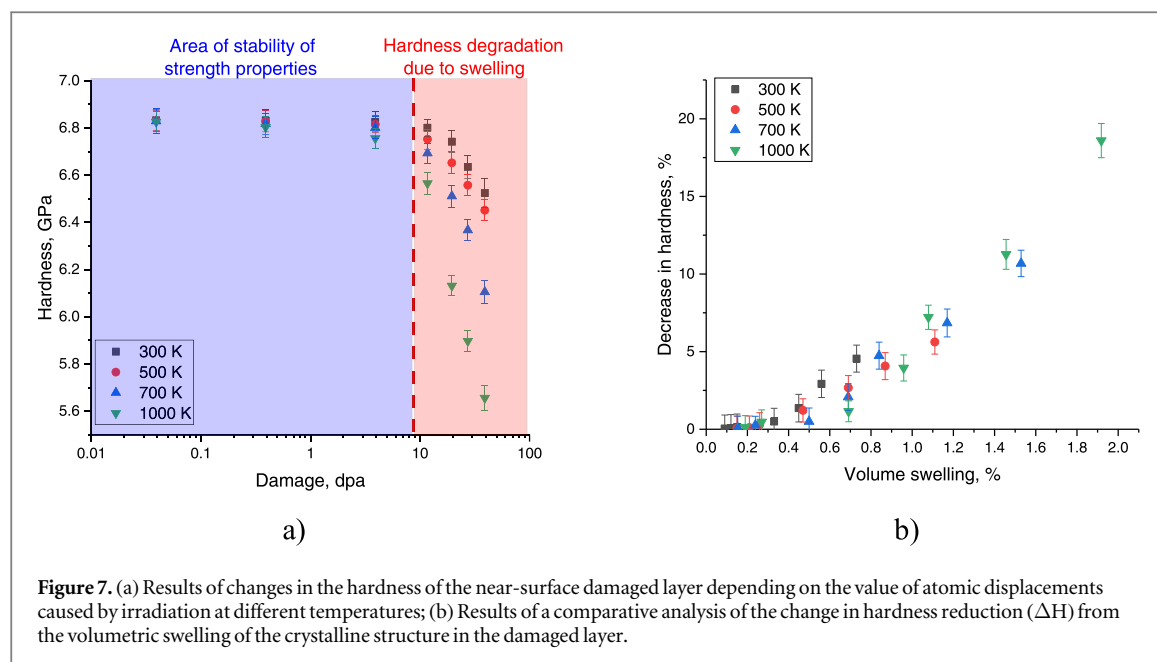


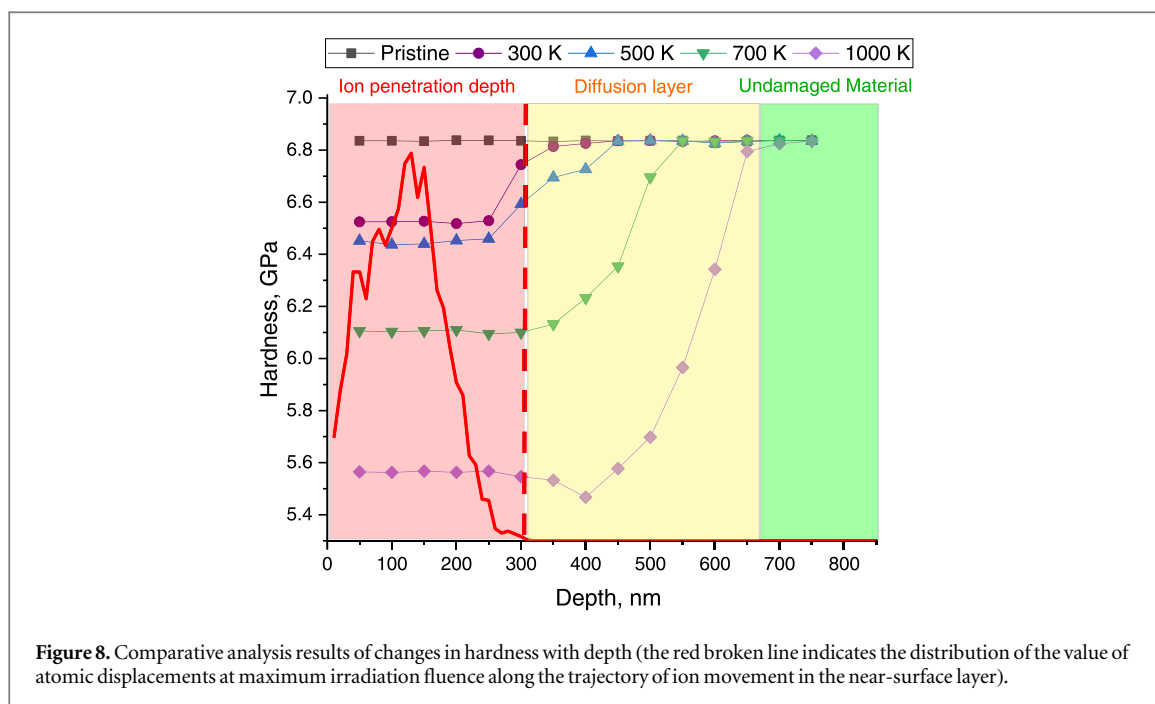
Figure 7. (a) Results of changes in the hardness of the near-surface damaged layer depending on the value of atomic displacements caused by irradiation at different temperatures; (b) Results of a comparative analysis of the change in hardness reduction (ΔH) from the volumetric swelling of the crystalline structure in the damaged layer.

FWHM value at fluences above 10^{17} ion cm^{-2} does not have a direct relationship to an increase with a change in fluence, which indicates a fairly high resistance of the alloy to amorphization under high-dose irradiation at low temperatures. Such effects may be due to the fact that at an irradiation temperature of 300 K, thermal effects leading to accelerated diffusion of implanted ions and resulting defects do not have a significant effect, since they arise only in areas near the trajectory of ion movement in the material, and by their nature have a short exposure time (about 10^{-11-13} s), which in the case of refractory alloys cannot lead to significant changes in the thermal vibrations of atoms. In the case of irradiation at high temperatures (about 700–1000 K), long-term thermal effects on the crystal structure, combined with ionization effects caused by irradiation, can result in an acceleration of diffusion processes, which in turn leads to enlargement of the blisters (see data presented in figure 3), and as a consequence, results in their destruction, which is accompanied by deformation destruction of the near-surface layer. Such destruction leads to the appearance of highly distorted structural inclusions in the damaged layer, the accumulation of which results in partial amorphization of the damaged layer, direct evidence of which is a steep rise in the FWHM value and a decrease in the intensity of diffraction reflections, the combination of changes of which indicates amorphization of the damaged layer.

Figure 7(a) demonstrates the results of measuring the hardness of the alloy samples under study depending on the magnitude of atomic displacements associated with changes in irradiation fluence, as well as reflecting the softening effect caused by structural changes in the near-surface layer. The hardness measurement was carried out with a sample in such a way that the data obtained during the measurements reflected the change in the hardness of the damaged layer at a given depth. The general trend of changes in the hardness of the surface layer indicates a cumulative effect characterizing the resistance of the alloy to softening under high-dose irradiation. Moreover, according to the data obtained, the change in hardness at atomic displacement values greater than 3 dpa in the case of irradiation temperature growth indicates an adverse effect of temperature on the softening rate. In the case of samples irradiated at temperatures of 300–500 K, a decrease in hardness is not observed until the accumulation of atomic displacements of the order of 10 dpa, and in the case of above 10 dpa, the decrease in hardness is less than 5%. For samples irradiated at temperatures of 700–1000 K, the hardness reduction is more pronounced with high-dose irradiation, which indicates a loss of strength properties of the near-surface layer of the alloys. A comparative analysis of the softening value (ΔH) and the swelling value (ΔV), presented in figure 6(b), shows a direct connection between strain swelling caused by irradiation and softening (decrease in hardness) of the near-surface layer, which is most pronounced during high-temperature irradiation.

Figure 8 illustrates the assessment results of changes in the hardness of the damaged layer in the alloy along the depth of penetration of ions in the material, performed by indentating the cross section of samples irradiated with a maximum fluence of 10^{18} ion cm^{-2} (for this experiment). The main goal pursued in conducting these experiments is to determine the diffusion mechanisms of defect propagation in the damaged layer in depth, as well as to determine the isotropy of changes in hardness depending on irradiation conditions.

According to the presented data of a comparative analysis of changes in hardness along the profile of the depth of penetration of ions into the near-surface layer depending on the irradiation temperature, it can be concluded that the temperature factor of irradiation has a negative effect on the diffusion mechanisms that



contribute to the softening of the near-surface layer. The data obtained indicate that with irradiation temperature growth, the depth of the softened layer (the layer in which the hardness value is lower than in the non-irradiated material) increases, and in the case of high-temperature irradiation it is practically twice the thickness of the layer characteristic of the ion travel depth. This effect can be explained by diffusion mechanisms associated with the high mobility of helium and its low solubility, which in turn leads to the fact that implanted helium can migrate quite well both in the damaged layer and beyond due to mobility. At the same time, it was shown in [31] that the mechanisms of helium diffusion in the surface layer are influenced by several factors, including the value of structural distortions that can restrain diffusion processes, as well as the concentration of defective inclusions during high-dose irradiation, which can also have a restraining effect in the form of dislocation or vacancy barriers.

Thus, analyzing the obtained data on changes in hardness with depth, we can conclude that diffusion processes, clearly expressed at high irradiation temperatures, have a negative impact not only on the overall decrease in strength characteristics, but also contribute to an increase in the thickness of the damaged layer due to migration processes. Similar effects associated with diffusion softening mechanisms, which contribute to an increase in the thickness of the damaged layer, should be taken into account when designing the use of such alloys under conditions of high-temperature radiation exposure.

Figure 9 demonstrates the measurement results of tribological characteristics, in particular, the dynamic change in the coefficient of dry friction under mechanical action on the surface with a ball-shaped indenter under load. The presented data characterizes the resistance of the surface to wear under mechanical influences.

The general trend of the presented dependences of the dynamics of alterations in the dry friction coefficient contingent upon irradiation conditions (with variations in irradiation fluence and irradiation temperature) indicates that the main changes associated with a decline in wear resistance (expressed in the friction coefficient growth and, as a consequence, the surface friction resistance growth) are observed at fluences above 3×10^{17} ion cm^{-2} . At the same time, the nature of changes in the friction coefficient at irradiation fluences in the range from 3×10^{17} to 10^{18} ion cm^{-2} has a clear trend toward a rise in the friction coefficient associated with temperature exposure.

The rise in the dry friction coefficient for high-dose irradiation in the case of high irradiation temperatures is due to a high softening degree of the near-surface layer (more than 10%–15% according to data on changes in hardness), which, as a consequence, is accompanied by an increase in the concentration of defective inclusions and deformation distortions, which, as a result of external influences, result in surface embrittlement and the creation of additional obstacles, leading to heightened resistance to friction and wear (see data in figure 10). It should be noted that the most pronounced changes in the dry friction coefficient are observed for samples irradiated at temperatures of 700–1000 K, for which high-dose irradiation leads to an increase in wear by more than 1.5–2 times compared to samples irradiated at temperatures of 300–500 K.

Analyzing the general trends in changes in hardness and wear resistance (based on the results of changes in the dry friction coefficient), the following conclusions can be drawn. Firstly, the data obtained, regardless of the

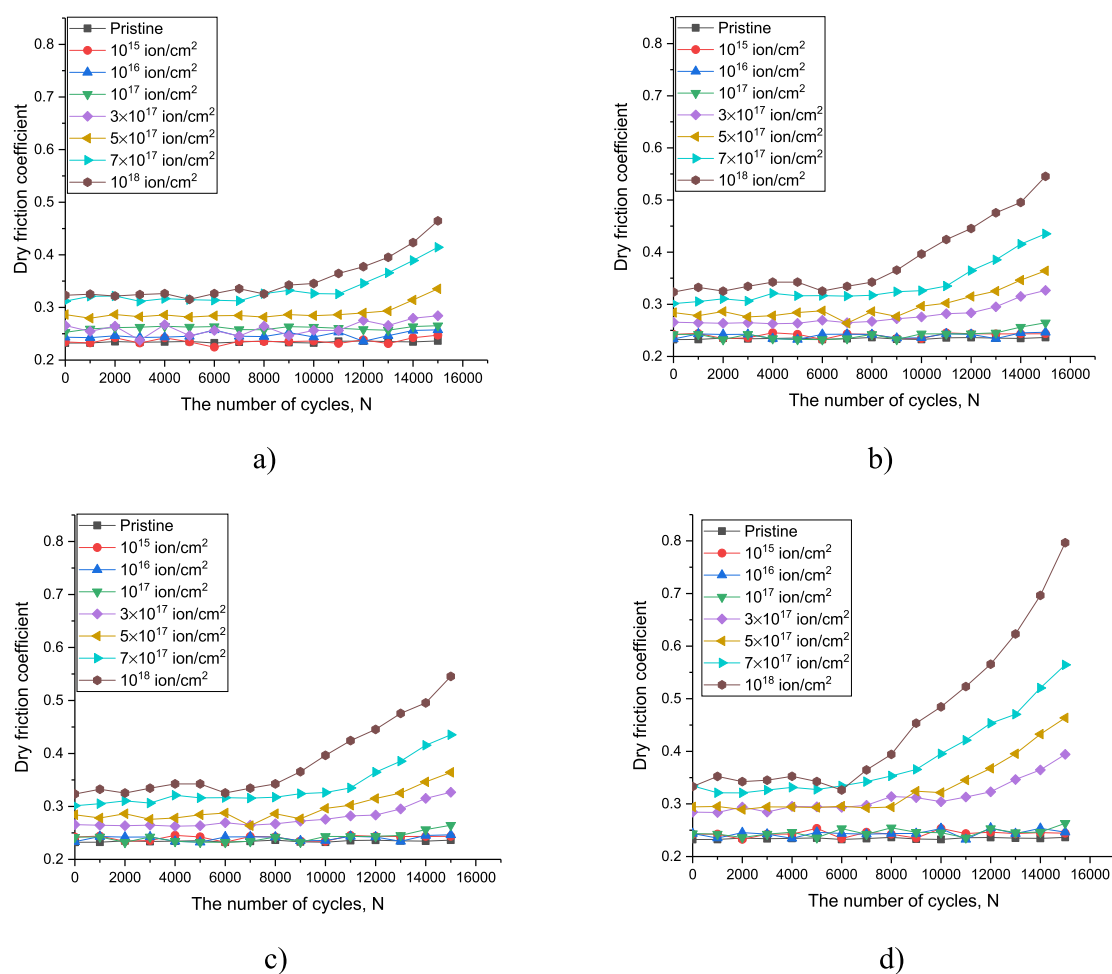


Figure 9. Results of tribological tests of the surface of the studied TiTaNbV alloys depending on the conditions of external influences associated with irradiation with He^{2+} ions with variations in irradiation temperature: (a) 300 K; (b) 500 K; (c) 700 K; (d) 1000 K.

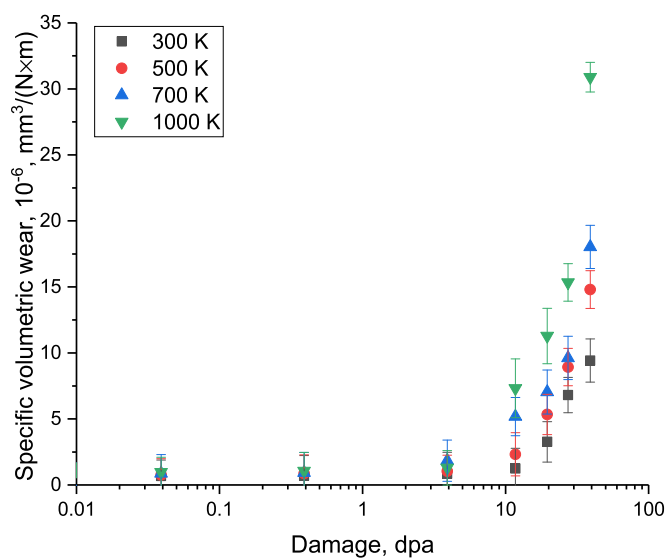


Figure 10. Comparative analysis results of the surface wear value depending on the atomic displacement value with varying irradiation conditions.

irradiation conditions (irradiation temperature), indicate a fairly high stability of the strength of the near-surface layer in the case of moderate irradiation fluences (up to 10^{17} ion cm^{-2}), characteristic of atomic displacement values of the order of 3–4 dpa. In this case, low radiation doses do not have a significant negative effect on the softening of the near-surface layer, and high stability indicators can be due to the structural features of high-entropy alloys. Secondly, the established connection between the softening of the near-surface layer and volumetric swelling caused by the accumulation of structural distortions indicates that the main mechanisms causing a reduction in strength characteristics are associated with the formation of highly disordered or amorphous inclusions in the damaged layer. At the same time, an increase in the size of the blisters in the case of high irradiation temperatures (700–1000 K) results in more pronounced softening and loss of wear resistance, which is caused by partial peeling of the damaged layer in the places of detonation opening of the blisters with the accumulation of excess concentrations of implanted helium in the gas-filled pore. Thirdly, an increase in irradiation temperature, as shown by wear resistance tests, leads not only to a decrease in wear resistance, but also to an increase in the depth of the damaged layer due to diffusion processes, leading to a more than twofold increase in the thickness of the deformation-softened near-surface layer.

Analyzing the obtained dependences of changes in the strength properties of the studied TiTaNbV alloys depending on the conditions of irradiation with low-energy helium ions, the following conclusions can be drawn. In comparison with multilayer MeN/Si₃N₄ films [32], in which the effect of gas swelling is reduced due to the presence of interphase boundaries, and the blistering effect itself is less pronounced, in the case of the alloys under study, the degradation of the near-surface layer is more pronounced, and also has a direct dependence on the irradiation temperature. Moreover, in the case of using these alloys as structural materials for nuclear reactors, high-entropy alloys have significant advantages over traditional stainless steels [33–35], which are less resistant to helium blistering, especially at elevated operating temperatures, at which accelerated migration of helium and enlargement of gas-filled inclusions occurs, followed by detonation opening.

One of the explanations for the effect of helium agglomeration with the subsequent formation of gas-filled inclusions in the near-surface layer is the Evans model [36, 37], proposed by him for steels and alloys, which also found good agreement in both multilayer films [32, 38] and ceramic materials [39–41]. The model proposed by Evans is based on the high mobility of helium and its low solubility, which leads to the fact that implanted helium in the near-surface layer migrates quite well along the grain boundaries, followed by filling the voids. Moreover, the possibility of its agglomeration at high concentrations of implanted helium can lead to the emergence of sufficiently large values of internal tensile stresses, the increase of which results in deformation swelling of these areas with their subsequent displacement to the surface. At the same time, in several works [42–44] it was indicated that a rise in irradiation temperature leads to an elevation in the mobility of implanted helium, and therefore, a more pronounced deformation distortion of the structure and volumetric growth of gas-filled cavities, which is in good agreement with the results presented in this work.

In comparison with ceramic materials [45–47] based on refractory compounds, high-entropy alloys benefit due to their thermophysical parameters, although a number of ceramics have a hardness significantly higher than the hardness of alloys. At the same time, during comparison of the results of helium swelling for the studied TiTaNbV alloys with other types of alloys, such as CrMoTaWV [48], Fe₅₀Mn₃₀Co₁₀Cr₁₀ [49], W-Ta-Cr-V [50], the observed changes in strength and structural parameters have similar dependencies. However, the TiTaNbV alloys under study have a more resistant structure to radiation-induced degradation processes caused by helium swelling under high-dose irradiation.

4. Conclusion

The paper presents the comprehensive analysis results of the relationship between changes in the structural and strength properties of refractory high-entropy TiTaNbV alloys to helium swelling with varying irradiation condition variation (in the case of irradiation temperature). Using the methods of scanning electron microscopy and x-ray diffraction analysis, the main structural disorder mechanisms, associated with the accumulation of deformation tensile stresses and microdistortions resulting from the agglomeration and enlargement of blisters in the near-surface layer, alongside their detonation hiding at high irradiation temperatures, were established.

During determination of the strength characteristics of the alloys under study depending on the irradiation conditions, it was found that the main changes due to the cumulative effect of helium implantation into the near-surface layer are observed at fluences above 10^{17} ion cm^{-2} . At the same time, an elevation in irradiation temperature results in more pronounced decrease in the hardness and wear resistance of the near-surface layer, which in turn implies a greater mobility of implanted helium in the near-surface layer due to high temperatures, which in turn leads to softening associated with the agglomeration of helium in voids. It should also be highlighted that irradiation temperature growth initiates diffusion mechanisms, which in turn results in softening of the near-surface layer to a greater depth under high-dose irradiation.

Data availability statement

No new data were created or analysed in this study.

Author contributions

Conceptualization, S G G, V V U, D I S, D B B, K K K, and A L K; methodology, V V U, S G G, and A L K; formal analysis, D I S, and A L K; investigation, S G G, V V U, K K K, D I S, and A L K; resources, A L K; writing—original draft preparation, review, and editing, S G G, D I S and A L K; visualization, S G G, A L K; supervision, A L K All authors have read and agreed to the published version of the manuscript.

Funding

This research was funded by the Science Committee of the Ministry of Education and Science of the Republic of Kazakhstan (No. BR18574135).

Institutional review board statement

Not applicable.

Informed consent statement


Not applicable.

Conflicts of interest

The authors declare no conflicts of interest.

ORCID iDs

Kayrat K Kadyrzhanov  <https://orcid.org/0009-0001-5462-0630>

Artem L Kozlovskiy  <https://orcid.org/0009-0005-4473-617X>

References

- [1] Saito S 2010 Role of nuclear energy to a future society of shortage of energy resources and global warming *J. Nucl. Mater.* **398** 1–9
- [2] Vaillancourt K, Labriet M, Loulou R and Waaub J P 2008 The role of nuclear energy in long-term climate scenarios: an analysis with the World- TIMES model *Energy Policy* **36** 2296–307
- [3] Brook B W, Alonso A, Meneley D A, Misak J, Blees T and van Erp J B 2014 Why nuclear energy is sustainable and has to be part of the energy mix *Sustain. Mater. Technol.* **1** 8–16
- [4] Zhan L, Bo Y, Lin T and Fan Z 2021 Development and outlook of advanced nuclear energy technology *Energy Strategy Reviews* **34** 100630
- [5] Buongiorno J, Corradini M, Parsons J and Petti D 2019 Nuclear energy in a carbon-constrained world: big challenges and big opportunities *IEEE Power Energ. Mag.* **17** 69–77
- [6] Was G S, Petti D, Ukai S and Zinkle S 2019 Materials for future nuclear energy systems *J. Nucl. Mater.* **527** 151837
- [7] Kadak A C 2005 A future for nuclear energy: pebble bed reactors *Int. J. Crit. Infrastruct.* **1** 330–45
- [8] Cheng Z, Sun J, Gao X, Wang Y, Cui J, Wang T and Chang H 2023 Irradiation effects in high-entropy alloys and their applications *J. Alloys Compd.* **930** 166768
- [9] Kareer A, Waite J C, Li B, Couet A, Armstrong D E J and Wilkinson A J 2019 Low activation, refractory, high entropy alloys for nuclear applications *J. Nucl. Mater.* **526** 151744
- [10] Shi T, Lei P H, Yan X, Li J, Zhou Y D, Wang Y P and Lu C Y 2021 Current development of body-centered cubic high-entropy alloys for nuclear applications *Tungsten* **3** 197–217
- [11] Wang X, Huang H, Shi J, Xu H Y and Meng D Q 2021 Recent progress of tungsten-based high-entropy alloys in nuclear fusion *Tungsten* **3** 143–60
- [12] Tunes M A, Fritze S, Osinger B, Willenshofer P, Alvarado A M, Martinez E and El-Atwani O 2023 From high-entropy alloys to high-entropy ceramics: the radiation-resistant highly concentrated refractory carbide (CrNbTaTiW) C *Acta Mater.* **250** 118856
- [13] Ayyagari A, Sallloom R, Muskeri S and Mukherjee S 2018 Low activation high entropy alloys for next generation nuclear applications *Materialia* **4** 99–103
- [14] El-Atwani O, Alvarado A, Unal K, Fensin S, Hinks J A, Greaves G and Martinez E 2021 Helium implantation damage resistance in nanocrystalline W-Ta-V-Cr high entropy alloys *Materials Today Energy* **19** 100599

- [15] Lu Y, Huang H, Gao X, Ren C, Gao J, Zhang H and Li T 2019 A promising new class of irradiation tolerant materials: Ti₂ZrHfV_{0.5}Mo_{0.2} high-entropy alloy *J. Mater. Sci. Technol.* **35** 369–73
- [16] Zhang W, Tang R, Yang Z B, Liu C H, Chang H, Yang J J and Liu N 2018 Preparation, structure, and properties of high-entropy alloy multilayer coatings for nuclear fuel cladding: a case study of AlCrMoNbZr/(AlCrMoNbZr) *N. J. Nucl. Mater.* **512** 15–24
- [17] Şimşek T, Kavaz E, Güler Ö, Şimşek T, Avar B, Aslan N and Tekin H O 2023 FeCoNiMnCr high-entropy alloys (HEAs): synthesis, structural, magnetic and nuclear radiation absorption properties *Ceram. Int.* **49** 25364–70
- [18] Yang T, Xia S, Liu S, Wang C, Liu S, Fang Y and Wang Y 2016 Precipitation behavior of Al_xCoCrFeNi high entropy alloys under ion irradiation *Sci. Rep.* **6** 32146
- [19] Chen W Y, Liu X, Chen Y, Yeh J W, Tseng K K and Natesan K 2018 Irradiation effects in high entropy alloys and 316H stainless steel at 300 °C *J. Nucl. Mater.* **510** 421–30
- [20] Qian L, Bao H, Li R and Peng Q 2022 Atomistic insights of a chemical complexity effect on the irradiation resistance of high entropy alloys *Materials Advances* **3** 1680–6
- [21] Xia S Q, Zhen W A N G, Yang T F and Zhang Y 2015 Irradiation behavior in high entropy alloys *Journal of Iron and Steel Research, International* **22** 879–84
- [22] George E P, Raabe D and Ritchie R O 2019 High-entropy alloys *Nature Reviews Materials* **4** 515–34
- [23] Giniyatova S G et al 2023 Study of the mechanisms of radiation softening and swelling upon irradiation of TiTaNbV Alloys with He²⁺ ions with an Energy of 40 keV *Materials* **16** 4031
- [24] Fang Q, Peng J, Chen Y, Li L, Feng H, Li J and Liaw P K 2021 Hardening behaviour in the irradiated high entropy alloy *Mech. Mater.* **155** 103744
- [25] Bollinger R K, White B D, Neumeier J J, Sandim H R Z, Suzuki Y, Dos Santos C A M and Betts J B 2011 Observation of a martensitic structural distortion in V, Nb, and Ta *Phys. Rev. Lett.* **107** 075503
- [26] Kita K and Hatmanto A D 2018 Significant structural distortion in the surface region of 4H-SiC induced by thermal oxidation and recovered by Ar annealing *ECS Trans.* **86** 63
- [27] Dobmann G, Korshunov S N, Kroening M, Martynenko Y V, Skorlupkin I D and Surkov A S 2008 Helium and radiation defect accumulation in metals under stress *Vacuum* **82** 856–66
- [28] Binyukova S Y, Chernov I I, Kalin B A, Kalashnikov A N and Timofeev A A 2002 Formation of gas pores in nickel alloys and structural steel under irradiation by helium ions *At. Energy* **93** 569–77
- [29] Sohatsky A S, Skuratov V A, Van Vuuren A J, Van Tiep N, O'Connell J H, Ibraeva A and Petrovich S 2019 Helium in swift heavy ion irradiated ODS alloys *Nucl. Instrum. Methods Phys. Res., Sect. B* **460** 80–5
- [30] Chen D, Zhao S, Sun J, Tai P, Sheng Y, Zhao Y and Kai J J 2019 Diffusion controlled helium bubble formation resistance of FeCoNiCr high-entropy alloy in the half-melting temperature regime *J. Nucl. Mater.* **526** 151747
- [31] Anderson A J, van Soest M C, Hodges K V and Hanchar J M 2020 Helium diffusion in zircon: effects of anisotropy and radiation damage revealed by laser depth profiling *Geochim. Cosmochim. Acta* **274** 45–62
- [32] Uglov V V et al 2020 Tolerance of MeN/Si₃N₄ (Me = Zr, Al, Cr) multilayered systems to radiation erosion *Surf. Coat. Technol.* **399** 126146
- [33] Borodin O V et al 2013 Synergistic effects of helium and hydrogen on self-ion-induced swelling of austenitic 18Cr10NiTi stainless steel *J. Nucl. Mater.* **442** S817–20
- [34] Klimenkov M, Möslang A and Materna-Morris E 2014 Helium influence on the microstructure and swelling of 9% Cr ferritic steel after neutron irradiation to 16.3 dpa *J. Nucl. Mater.* **453** 54–9
- [35] Liu C et al 2024 Cavity swelling of 15-15Ti steel at high doses by ion irradiation *Materials* **17** 925
- [36] Evans J H 1976 A mechanism of surface blistering on metals irradiated with helium ions *J. Nucl. Mater.* **61** 1–7
- [37] Evans J H and Van Veen A 1996 Gas release processes for high concentrations of helium bubbles in metals *J. Nucl. Mater.* **233** 1179–83
- [38] Uglov V V et al 2020 Surface blistering in ZrSiN nanocomposite films irradiated with He ions *Surf. Coat. Technol.* **394** 125654
- [39] Abyshev B et al 2022 Study of radiation resistance to helium swelling of Li₂ZrO₃/LiO and Li₂ZrO₃ ceramics *Crystals* **12** 384
- [40] Ryazanov A I et al 2004 Effect of helium on radiation swelling of SiC *Phys. Scr.* **2004** 195
- [41] Kozlovskiy A L 2021 Determination of critical doses of radiation damage to AlN ceramic under irradiation of helium and hydrogen ions *Eurasian Physical Technical Journal* **18** 23–8
- [42] Zhang W et al 2024 Temperature-dependent swelling in helium ion irradiated vanadium *Nucl. Technol.* **1** 1–7
- [43] Trinkaus H 1985 Modeling of helium effects in metals: high temperature embrittlement *J. Nucl. Mater.* **133** 105–12
- [44] Katoh Y, Kishimoto H and Kohyama A 2002 The influences of irradiation temperature and helium production on the dimensional stability of silicon carbide *J. Nucl. Mater.* **307** 1221–6
- [45] Kislitsin S B et al 2020 Degradation processes and helium swelling in beryllium oxide *Surf. Coat. Technol.* **386** 125498
- [46] Zinkle S J 2012 Effect of H and He irradiation on cavity formation and blistering in ceramics *Nucl. Instrum. Methods Phys. Res. B* **286** 4–19
- [47] Huang Z et al 2019 Defect-fluorite Gd₂Zr₂O₇ ceramics under helium irradiation: amorphization, cell volume expansion, and multi-stage bubble formation *J. Am. Ceram. Soc.* **102** 4911–8
- [48] Cheng T et al 2023 Enhanced resistance to helium irradiations through unusual interaction between high-entropy-alloy and helium *Acta Mater.* **248** 118765
- [49] Su Z et al 2022 The effect of interstitial carbon atoms on defect evolution in high entropy alloys under helium irradiation *Acta Mater.* **233** 117955
- [50] El-Atwani O et al 2021 Helium implantation damage resistance in nanocrystalline W-Ta-V-Cr high entropy alloys *Materials Today Energy* **19** 100599